

Chaotic behavior of a random laser with static disorder

Sushil Mujumdar,^{*} Volker TÜRCK, Renato Torre, and Diederik S. Wiersma[†]

European Laboratory for Non-linear Spectroscopy, INFN-BEC, and Phys. Dept., University of Florence, Sesto Fiorentino, Italy

(Received 12 February 2007; published 7 September 2007)

We report on an experimental and numerical study of chaotic behavior in random lasers. The complex emission spectra from a disordered amplifying material with static disorder are investigated in a configuration with controlled, stable experimental conditions. It is found that, upon repeated identical excitation, the emission spectra are distinct and uncorrelated. This behavior can be understood in terms of strongly coupled modes that are triggered by spontaneous emission, and is expected to play an important role in most pulsed random lasers.

DOI: [10.1103/PhysRevA.76.033807](https://doi.org/10.1103/PhysRevA.76.033807)

PACS number(s): 42.55.Zz, 42.25.Dd, 42.25.Hz

I. INTRODUCTION

Light transport in disordered systems has fascinating analogies with electron transport [1] and the transport of cold atom gases [2]. Phenomena like universal conductance fluctuations of light [3], optical weak [4] and strong (Anderson) localization [5], optical Bloch oscillations, and Zener tunneling [6] have all been observed in recent years. A particularly interesting situation arises when optical gain is added to a random material. If the total gain becomes larger than the losses, these systems become unstable and exhibit a lasing threshold. The simplest description of lasing in random systems is based on a diffusion equation with gain, which leads to the notion of a critical volume above which gain is larger than loss [7]. This simplified description can already describe several of the observations done on amplifying random materials, including powders, laser dye suspensions, and organic systems [8–12]. Theoretically, this phenomenon has furthermore been treated analytically [13–15], through Monte Carlo simulations [16–18], by finite-difference time-domain calculations [19], and by using random matrix theory [20]. The behavior of such system shows several analogies with a regular laser, including gain narrowing, laser spiking, and relaxation oscillations [8,15].

The general spectral signature of random lasing is an overall narrowing of the emission spectrum. In addition to this observation, there have been experiments in which more complex emission spectra are observed, containing a fascinating collection of spectrally narrow peaks. Such spectra were first observed on zinc oxide powders and later also on other materials [21–23]. These observations have triggered a discussion about the possibility of lasing of Anderson localized modes in random systems. Anderson localization is an interference phenomenon that occurs in very strongly scattering media and that leads to the formation of localized modes that are exponentially confined in space [5]. Due to this exponential confinement, these modes have potentially a high lifetime and quality factor which means that they are very suitable for obtaining lasing [24,25]. In practice, it is

difficult to obtain Anderson localization in three-dimensional disordered systems due to the extremely strong scattering that is required. Since narrow emission spikes were also observed in the diffusive scattering regime far away from Anderson localization, a different explanation had to be found.

Alternative explanations for the observation of narrow emission spikes in random lasers have been put forward [26], like the possibility of having “anomalously localized states” in the diffusive regime [27–29]. We have recently proposed an interpretation of the complex random laser emission spectra without the requirement of localization, based on the amplification of statistically rare long light paths in random systems [30]. This idea was confirmed in recent numerical calculations showing that lasing can indeed be obtained in extended modes with a long lifetime, and that random lasing does not necessarily require Anderson localization [31]. The threshold of random lasers was found to show strong fluctuations, depending on the pulse duration of the excitation laser [32], which inspired a study on fluctuations in random lasers with dynamic disorder (e.g., particles in solution) [33].

Most experimental and theoretical studies on random lasing with spectrally narrow features have assumed that the narrow spikes in the emission spectrum can be directly associated with the mode structure of the laser. Narrow spikes have been observed in several cases on materials with *static* disorder, i.e., samples that do not change their configuration over time. In that case, one might naively expect the spectrum to be reproducible upon repetition of the experiment. In the study reported in this paper, we have examined the reproducibility of random laser spectra with spectrally narrow features. We observe that such spectra can be surprisingly unstable and exhibit a strongly chaotic behavior. We optically excite a random laser material with static disorder in a pulsed configuration, and analyze individual single-pulse emission spectra. We observe that successive emission spectra are entirely uncorrelated for our choice of parameters. Hence the system lases in different modes in successive excitation events, while the sample disorder and other system parameters are constant.

This paper is organized as follows. In Sec. II, we will explain the sample preparation technique and experimental configuration. In Sec. III, we show the results of the experiments on emission spectra. In Sec. IV, we report experimental data on the speckle patterns observed from these samples.

^{*}Present address: Tata Institute of Fundamental Research, Mumbai, India. mujumdar@tifz.zer.in

[†]wiersma@lens.unifi.it; <http://www.complexphotonics.org>

In Sec. V, we report on Monte Carlo simulations performed on these systems and, in Sec. VI, we discuss the interpretation of the results and their relation to lasing mechanisms in random systems above threshold.

II. SAMPLES AND EXPERIMENTAL SETUP

The sample with static disorder was made from SK11 (Schott) glass. A fine powder of the glass was obtained by grinding in a planetary micromill. The powder was chemically cleaned and sintered under a pressure of 1.2 GPa to obtain robust porous disks of 1 cm diameter and 6 mm thickness. The porosity of the sample enabled us to infiltrate it with a solution of rhodamine-6G in methanol (molar concentration 5×10^{-3} mol/l). The mean free path of the sample, indicated as ℓ in the subsequent text, was found to be $50 \mu\text{m}$ as determined from the measurement of the diffusion constant.

To determine the amount of disorder in a random material, the parameter $k\ell$ is commonly used, with $k=2\pi/\lambda$ being the magnitude of the wave vector. This parameter reflects the comparison between the mean free path and the wavelength. Note that strong scattering corresponds to small values of $k\ell$. Anderson localization of optical waves is expected to occur when the mean free path becomes comparable to the wavelength and, in particular, when $k\ell \leq 1$ [5]. Effects related to Anderson localization can also play a role around $k\ell=1$. In this regime, finite-size effects lead to scaling of the transport parameters [34], i.e., the transport parameters like the mean free path and diffusion constant depend on the sample size.

For our samples, we have $k\ell=5.4 \times 10^2$, for the central wavelength of the emission band. The samples are therefore clearly far out of the Anderson localization regime. Optical excitation was provided by the frequency-doubled output ($\lambda=532.8 \text{ nm}$) of a mode-locked neodymium-doped yttrium aluminum garnet (Nd:YAG) laser (2.5 Hz repetition rate, 25 ps pulse width), focused on the sample surface in a spot of $100 \mu\text{m}$ diameter. From previous calculations [15], we know that the pump intensity is expected to fall off nearly linearly inside the sample, with the mean free path (in our case $50 \mu\text{m}$) as the characteristic length scale. A Peltier-cooled charge-coupled device CCD array coupled to a monochromator was synchronized with the laser pulses to record single-shot emission spectra. The emission from the illuminated sample surface was collected by a collection lens with a focal length of 6 cm and numerical aperture 0.39, placed under an angle of 30° with the sample normal. The spectral resolution of the setup was measured using a calibrated mercury lamp and was found to be below 0.2 nm.

III. EMISSION SPECTRA

Figure 1 shows experimentally observed single-shot emission spectra from the sample for three successive pulses of the excitation laser (excitation energy $1.2 \mu\text{J}$, corresponding to a peak intensity of $6.1 \times 10^8 \text{ W/cm}^2$). In each of the spectra, a broadband profile (pedestal) is observed. High-intensity ultranarrow spikes are seen imposed on the broad pedestal. The bandwidth of the narrowest spike is below 0.2 nm

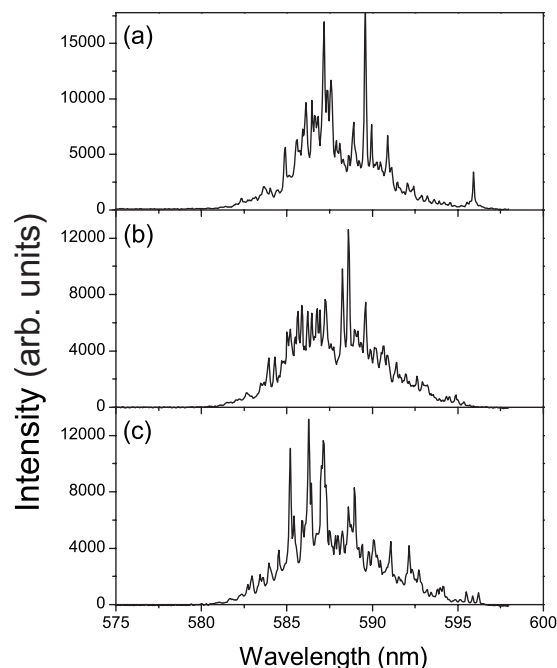


FIG. 1. Experimentally observed single-shot emission spectra from a porous glass disk infiltrated with Rhodamine 6G. The mean free path of the sample was $50 \mu\text{m}$. The three spectra shown are taken at three successive excitation pulses. The spectrally narrow emission spikes occur at different wavelengths from pulse to pulse.

($\sim 0.15 \text{ nm}$). Clearly, the locations of the high-intensity spikes in each spectrum are different from shot to shot, and neither are they equispaced.

We find that the occurrence of the emission spikes is strongly nonlinear with excitation energy, and exhibits a threshold behavior. In Fig. 2, the average height of the sharp emission peaks is plotted versus excitation energy. At every pump energy, a minimum of 100 single-shot emission spectra were collected. For every spectrum, the intensity of each spike was measured relative to the broad pedestal, and the

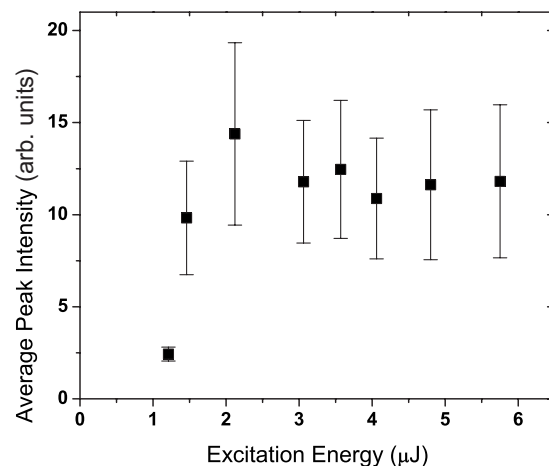


FIG. 2. Average intensity of the observed narrow emission spikes versus excitation energy. Below an excitation energy of $1.2 \mu\text{J}$, no narrow spikes were observed; hence their height is zero.

average peak height was calculated. This was done for all the spectra in the set for a given pump energy. The total average was found and is plotted in Fig. 2. Below an excitation energy of $1.2 \mu\text{J}$, no sharp peaks were observed; hence the peak height is zero for excitation energies below $1.2 \mu\text{J}$. The bars on the points give the standard deviation at each pump pulse. As can be seen, the fluctuations in the peak height are very large.

In case of a conventional laser cavity, wherein the amplifying medium is enclosed within a resonator, the modes would be equally spaced with a mode spacing given by the free spectral range $\Delta\nu$. Considering only one transverse mode, the longitudinal mode spacing of a regular Fabry-Perot resonator is $\Delta\lambda = \lambda_0^2/2L_c$, with L_c the cavity length. In our random system, on the other hand, the modes will be overlapping in wavelength. The number of modes N supported by our random system, at a specific wavelength λ , can be estimated from the surface area A that is emitting using $N = 2\pi A/\lambda^2$ [35]. For our sample this surface is at least the size of the area illuminated by the excitation laser, which is $7.8 \times 10^3 \mu\text{m}^2$, so that we have $N \geq 1.4 \times 10^5$. Out of this large number of modes, only a certain fraction of modes with the longest lifetime will eventually lase. However, this large number clearly indicates that strong mode competition can be expected in the random case.

IV. STATIC DISORDER

The single-shot emission spectra in Fig. 1 indicate a strongly chaotic behavior. To interpret this behavior correctly, it is important to verify that the disorder in the sample is indeed static. That is, the configuration of the scattering elements should be stable from shot to shot. Otherwise, the changes in the emission spectra could be attributed to a changing realization of the disorder or sample geometry. A classic indicator of relative scatterer positions is the speckle pattern generated by interference of multiply scattered waves. Since the speckle pattern is a direct consequence of the phases of waves that are multiply scattered throughout the random medium, it is extremely sensitive to any changes in the scatterer configuration. This sensitivity is applied in a technique called diffusing-wave spectroscopy to study nanometer-scale movements of particles with visible light [36]. A high sensitivity for the particle positions is obtained due to the multiple-scattering process. The speckle pattern changes when the cumulative phase shift induced by movements of the particles becomes comparable to the wavelength λ . A static speckle pattern can therefore be used to demonstrate that the configuration of the disorder in the sample is constant on length scales that are relevant for the optical properties of the sample. On the same grounds, one can expect a similar sensitivity to the stability of the entire experimental setup.

We monitored the speckle pattern generated by the sample to assess any variation in the disorder configuration. Accordingly, the speckle was realized by the multiple scattering of the excitation light ($\lambda = 532.8 \text{ nm}$). The CCD camera, employed in imaging mode, recorded the speckle pattern at individual laser shots. Two such speckle patterns are shown in

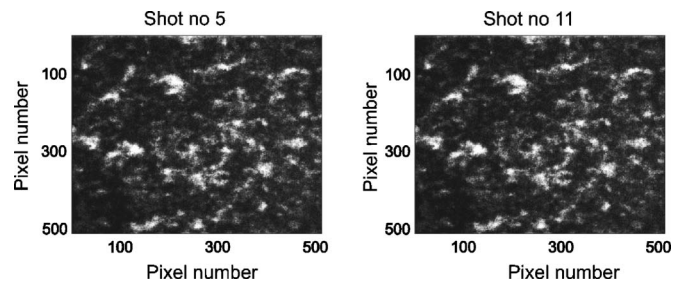


FIG. 3. Far-field speckle patterns observed from two distinct laser pulses (fifth and eleventh in a series of pulses). The numbers on the axes indicate pixels on the CCD array. The highly correlated intensity distribution confirms that the configuration of scatterers does not change over subwavelength length scales, even over several laser pulses. Hence the spatial mode distribution remains unchanged over several laser shots.

Fig. 3. Clearly, the two speckle patterns are nearly identical, demonstrating that the realization of the disorder is not changing. Minor visible differences between the two patterns arise from CCD noise, which is unavoidable. These patterns are spaced $\sim 2 \text{ s}$ in time. Typically, we found that the correlation in the speckle pattern persisted for much longer times and over many excitation shots. The strong correlation between individual speckle patterns rules out not only any variation in the scatterer configuration, but also fluctuations of the incident excitation beam or other forms of experimental instability.

A series of both spectral and speckle correlation measurements is reported in Fig. 4. Here, the correlation between the spectral profiles (circles) generated at successive laser pulses, and the correlation between the speckle patterns (squares) generated at successive laser pulses is plotted. The correlation was calculated in the standard way as the (Pearson's) linear correlation coefficient [37]. The correlation in the spectra was calculated after subtracting the broadband pedestal from each spectrum. For the speckle patterns, the correlation coefficient was calculated from corresponding pixel values of successive CCD images. From Fig. 4, we can see that the speckle pattern is highly correlated over several laser pulses, while the spectra are uncorrelated.

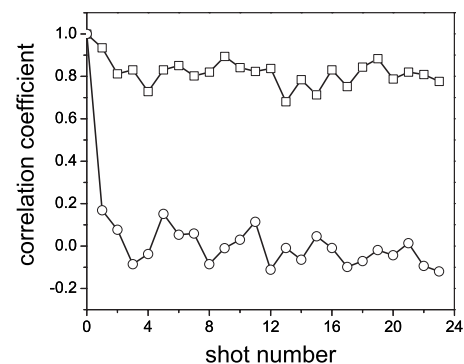


FIG. 4. Spectral (\circ markers) and speckle (\square markers) correlation coefficient over several laser pulses. Speckle patterns are highly correlated over several laser pulses, whereas the spectra are uncorrelated.

V. MONTE CARLO SIMULATIONS

The emission from such a system was modeled by a Monte Carlo simulation of photon migration in a random medium. In such an approach, the multiple-scattering process is mapped as a series of random walks [16]. The approach followed here takes into account the spontaneous emission of photons, or energy packets, by the excited dye molecules, the successive random walk of these energy packets through the disordered system, and the stimulated emission from excited dye molecules. In this context, the terminology “photon” is somewhat misleading, since the light field is not quantized in a quantum-mechanical sense, and hence the calculation is completely classical. It is therefore clearer to refer to energy packets, which have no temporal spread. During the simulation of sample excitation, an energy packet was taken as a collection of N units of energy at the pump wavelength, while, during fluorescence, it was a packet of *unit* energy, associated with a wavelength from the fluorescence spectrum of the dye. In either situation, it performed a random walk, whose characteristics such as the path length of ballistic traversal, direction of propagation, etc., were random variates chosen from the appropriate distribution. During the random walk, the local population dynamics of the ground and excited states of the material were kept track of, so that gain saturation was incorporated automatically in the form of a reduction of the local population inversion.

The simulation was adapted for static disorder in the following manner. Two disjoint vectors of random numbers were generated using two different seeds, one simulating the spontaneous emission process, and the other simulating light transport. The light transport seed remained unchanged at the start of each Monte Carlo run. This ensured that, once an energy packet was scattered into a certain channel, it traversed the same channel throughout its random walk for every laser shot, equivalent to the situation where the relative scatterer positions remain unchanged.

The excitation was calculated from the multiple-scattering process of an energy packet of wavelength $\lambda=532$ nm, which underwent absorption by the ground-state dye molecules. The absorption cross section of the molecules was taken to be $\sigma_{abs}=3.7 \times 10^{-16}$ cm², and the number of dye molecules was determined from the dye concentration. This excitation mechanism using the pump pulse of the requisite energy resulted in a population inversion, which was followed by fluorescence. The fluorescence was calculated as a collection of spontaneous emission events. The location of each event was calculated from the cumulative probability distributions constructed by using the spatial gain profile, which was the same for all laser pulses. The wavelength λ of the spontaneous emission event was determined from the normalized fluorescence spectrum of the dye and was subject to randomness (spontaneous emission). The requisite data on the absorption and fluorescence spectra of the dye sample were taken from available literature [38]. The energy packet generated in the spontaneous event performed a three-dimensional random walk through the active random medium, undergoing amplification through stimulated emission or reabsorption, depending upon local population inversion. Upon its exit, the resultant change in its energy was recorded

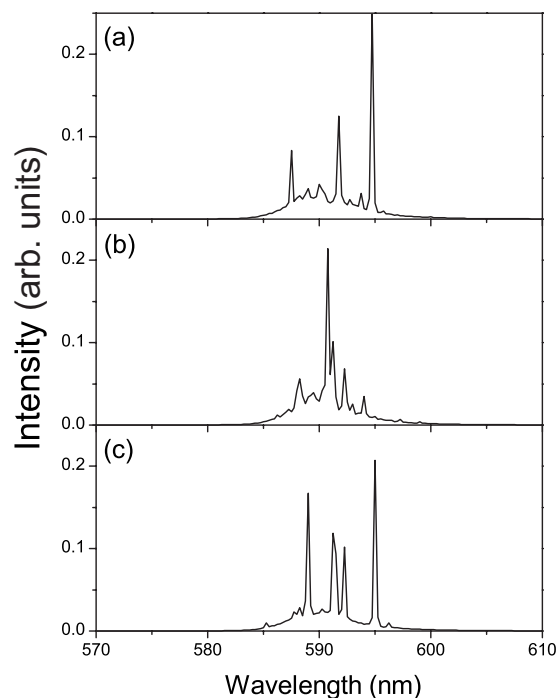


FIG. 5. Calculated emission spectra from a random laser with static disorder. The three panels are the emission spectra for three successive excitation pulses. The narrow lasing spikes, originating from statistically rare extended modes in the random system, are visible at different wavelengths in successive excitation pulses.

and the population inversion was accordingly revised. Subsequently, the next spontaneous emission was simulated, for which the emitted photon encountered a different gain environment in its propagation. Thus, the local gain coefficient experienced by every energy packet was varying, and was automatically accounted for in the simulation. These concurrent population dynamics ensured the inclusion of competition between different paths. From the recorded values of the wavelength of the energy packets, emission spectra were reconstructed for each individual laser pulse.

Figure 5 shows the calculated single-shot spectra for three different laser pulses calculated for the same sample geometry as in the experiment and an excitation energy of 1.46 μ J. Ultranarrow lasing peaks imposed on a broad spectrum are clearly observed. The bandwidth of each peak is 0.25 nm, equal to the spectral resolution maintained in the simulation. The broad background is a consequence of a large number of moderately amplified spontaneous emission events. The moderate amplification in this case is a result of their average path length inside the excited region. On the other hand, we observe that some spontaneous emission photons traverse certain light paths that are very long. The long paths of the photons illustrate that a fraction of the scattered light waves remains in the scattering medium for a long time and spans a significant volume of the excited sample. They are, therefore, representative of the long-lived, extended modes of the system. Due to their low statistical occurrence, they play no significant role in the transport at low or zero gain, but at or above threshold these events acquire so much gain that they dominate the spectrum in the form of narrow

emission spikes. The emission spectra are necessarily uncorrelated due to the random seed in the random number generator used for calculating the wavelength of the spontaneously emitted photon (appropriately normalized with the fluorescence curve of the gain material). This reflects the randomness in the spontaneous emission process, which lies at the origin of the observed chaotic behavior in shot-to-shot spectra.

Note that, while a Monte Carlo simulation provides information on the modes of a random system, the paths that are calculated are not the same as the optical modes. A light path, as calculated by the simulation, is a geometric entity with zero cross section that depicts the direction of propagation of a scattered wave. It gives an accurate estimate, however, of the time spent by a scattered wave inside the medium, and marks out the traversed region of the sample. We emphasize that the various simulation characteristics such as the scattering strength, the direction of propagation, etc., are statistical estimates based on exact Mie theory. Monte Carlo simulations, therefore, have been very successful to describe the transport of light in random systems. What is also included in a Monte Carlo simulation is the competition between modes by coupling via the gain medium. When a rare long path is triggered by spontaneous emission, the exponential gain leads to deexcitation of a significant volume of the sample. Other long paths that spatially overlap with this deexcited region then experience much less gain, which hampers their growth to the lasing threshold.

VI. INTERPRETATION

It is interesting to discuss the implications of the above experimental and numerical observations for the interpretation of random lasing. It is clear that the observed peaks are related to a strong chaotic behavior, in the sense that the emission spectrum is extremely sensitive to small fluctuations in the initial conditions. These fluctuations can be provided by the spontaneous emission process, which is the only element that is different and uncorrelated in successive emission events. Such chaotic behavior is observed also in regular lasers, especially in systems with a large number of coupled modes above threshold and for inhomogeneous cavities [39].

In our random system the number of optical modes is large, and there exists strong mode coupling if the modes are extended. Mode coupling takes place via the gain medium by competition for the available gain. Lasing in one specific

mode means that the population inversion will be rapidly deexcited in the volume occupied by this mode. Hence other modes that spatially overlap with this mode will experience a reduction of total gain. This mode competition can explain the observed sensitivity to the initial boundary conditions.

Our samples have a scattering strength that is nearly three orders less than the disorder required to obtain Anderson localization. Hence the results are valid in the diffusive regime. In the Anderson localization regime, on the other hand, one can expect a different behavior. Localized states are formed in distinct regions of the sample and, by their nature, have nearly zero spatial overlap. Hence the gain competition will be much less in the Anderson-localized case. Note that the diffusive regime does not imply that there is no interference in the samples. In all random dielectric materials studied in the context of random lasing, the phase is conserved in the scattering process; hence interference takes place. If the system is Anderson localized, the optical modes are exponentially confined, whereas if the system is diffusive the modes are extended. Such extended modes can lase if their lifetime is long enough.

VII. CONCLUSIONS

In conclusion, we have studied strongly chaotic behavior as observed in the emission spectra of random laser systems. The observations can be understood in terms of mode coupling between long-lived extended modes in a random laser. The chaotic behavior is inherent in the fluorescence of the amplifying random medium and is not related to the type of disorder in the system. Typical amplifying random media such as rhodamine- or zinc oxide-based disordered structures should therefore exhibit the same effects. In future studies, it would be interesting to explore the dependence of the observed chaotic behavior on relevant time scales like the duration of the excitation pulse, the fluorescence lifetime of the gain medium, and the diffusion time.

ACKNOWLEDGMENTS

We wish to thank Marilena Ricci for help with the experiments and Stefano Cavalieri, Roberto Livi, Stefano Lepri, and the complex photonic systems group at LENS for stimulating discussions. This work was financially supported by LENS under EC Contract No. RII3-CT-2003-506350, and by the EU through Network of Excellence "Phoremot" (Grant No. IST-2-511616-NOE). S.M. acknowledges the support of the TRIL program of the ICTP, Trieste.

-
- [1] P. Sheng, *Introduction to Wave Scattering, Localization, and Mesoscopic Phenomena* (Academic Press, San Diego, 1995).
 [2] H. Gimpelrein, S. Wessel, J. Schmiedmayer, and L. Santos, *Phys. Rev. Lett.* **95**, 170401 (2005); D. Clement, A. F. Varon, M. Hugbart, J. A. Retter, P. Bouyer, L. Sanchez-Palencia, D. M. Gangardt, G. V. Shlyapnikov, and A. Aspect, *ibid.* **95**, 170409 (2005); C. Fort, L. Fallani, V. Guarrera, J. E. Lye, M.

- Modugno, D. S. Wiersma, and M. Inguscio, *ibid.* **95**, 170410 (2005).
 [3] F. Scheffold and G. Maret, *Phys. Rev. Lett.* **81**, 5800 (1998).
 [4] Y. Kuga and A. Ishimaru, *J. Opt. Soc. Am. A* **1**, 831 (1984); M. P. Van Albada and A. Lagendijk, *Phys. Rev. Lett.* **55**, 2692 (1985); P. E. Wolf and G. Maret, *ibid.* **55**, 2696 (1985).
 [5] S. John, *Phys. Rev. Lett.* **53**, 2169 (1984); P. W. Anderson,

- Philos. Mag. B **52**, 505 (1985); D. S. Wiersma *et al.*, Nature (London) **390**, 671 (1997); A. A. Chabanov and A. Z. Genack, Phys. Rev. Lett. **87**, 153901 (2001); M. Störzer, P. Gross, C. M. Aegerter, and G. Maret, *ibid.* **96**, 063904 (2006).
- [6] M. Ghulinyan, C. J. Oton, Z. Gaburro, L. Pavesi, C. Toninelli, and D. S. Wiersma, Phys. Rev. Lett. **94**, 127401 (2005).
- [7] V. S. Letokhov, Zh. Eksp. Teor. Fiz. **53**, 1442 (1967) [Sov. Phys. JETP **26**, 835 (1968)].
- [8] C. Gouedard *et al.*, J. Opt. Soc. Am. B **10**, 2358 (1993).
- [9] V. M. Markushev, V. F. Zolin, and Ch. M. Briskina, Zh. Prikl. Spektrosk. **45**, 847 (1986).
- [10] N. M. Lawandy *et al.*, Nature (London) **368**, 436 (1994); W. L. Sha, C. H. Liu, and R. R. Alfano, Opt. Lett. **19**, 1922 (1994).
- [11] M. Bahoura, K. J. Morris, and M. A. Noginov, Opt. Commun. **201**, 405 (2002).
- [12] D. S. Wiersma and S. Cavalieri, Nature (London) **414**, 708 (2001).
- [13] A. Yu. Zyuzin, Europhys. Lett. **26**, 517 (1994).
- [14] S. John and G. Pang, Phys. Rev. A **54**, 3642 (1996).
- [15] D. S. Wiersma and A. Lagendijk, Phys. Rev. E **54**, 4256 (1996); D. S. Wiersma, Ph.D. thesis, University of Amsterdam, 1995.
- [16] G. A. Berger, M. Kempe, and A. Z. Genack, Phys. Rev. E **56**, 6118 (1997).
- [17] S. Mujumdar and H. Ramachandran, Opt. Commun. **176**, 31 (2000).
- [18] S. Mujumdar, S. Cavalieri, and D. S. Wiersma, J. Opt. Soc. Am. B **21**, 201 (2004).
- [19] Xunya Jiang and C. M. Soukoulis, Phys. Rev. Lett. **85**, 70 (2000).
- [20] C. W. J. Beenakker, Phys. Rev. Lett. **81**, 1829 (1998).
- [21] H. Cao, Y. G. Zhao, S. T. Ho, E. W. Seelig, Q. H. Wang, and R. P. H. Chang, Phys. Rev. Lett. **82**, 2278 (1999).
- [22] H. Cao, J. Y. Xu, S.-H. Chang and S. T. Ho, Phys. Rev. E **61**, 1985 (2000).
- [23] R. C. Polson, M. E. Raikh, and Z. V. Vardeny, IEEE J. Sel. Top. Quantum Electron. **9**, 120 (2003).
- [24] P. Pradhan and N. Kumar, Phys. Rev. B **50**, 9644 (1994).
- [25] V. Milner and A. Z. Genack, Phys. Rev. Lett. **94**, 073901 (2005).
- [26] Y. Sun, J. B. Ketterson, and G. K. L. Wong, Appl. Phys. Lett. **77**, 2322 (2000).
- [27] A. D. Mirlin, Phys. Rep. **326**, 259 (2000).
- [28] S. E. Skipetrov and B. A. van Tiggelen, Phys. Rev. Lett. **92**, 113901 (2004).
- [29] V. M. Apalkov, M. E. Raikh, and B. Shapiro, Phys. Rev. Lett. **89**, 126601 (2002).
- [30] S. Mujumdar, M. Ricci, R. Torre, and D. S. Wiersma, Phys. Rev. Lett. **93**, 053903 (2004).
- [31] C. Vanneste, P. Sebbah, and H. Cao, Phys. Rev. Lett. **98**, 143902 (2007).
- [32] D. L. Anglos *et al.*, J. Opt. Soc. Am. B **21**, 208 (2004).
- [33] K. L. van der Molen, A. P. Mosk, and A. Lagendijk, Phys. Rev. A **74**, 053808 (2006).
- [34] E. Abrahams, P. W. Anderson, D. C. Licciardello, and T. V. Ramakrishnan, Phys. Rev. Lett. **42**, 673 (1979).
- [35] J. H. Li and A. Z. Genack, Phys. Rev. E **49**, 4530 (1994).
- [36] G. Maret and P. E. Wolf, Z. Phys. B: Condens. Matter **65**, 409 (1987); D. J. Pine, D. A. Weitz, P. M. Chaikin, and E. Herbolzheimer, Phys. Rev. Lett. **60**, 1134 (1988).
- [37] H. Press *et al.*, *Numerical Recipes in C++* (Cambridge, New York, 2002).
- [38] Lambdachrom laser dyes, Lambda Physik, Lasertechnik, (1986).
- [39] A. E. Siegman, *Lasers* (University Science Books, Sausalito, CA, 1986); , Phys. Rev. A **39**, 1264 (1989); L. I. Deych, Phys. Rev. Lett. **95**, 043902 (2005).